

# A morphometric study of the amygdala in the guinea pig

Maciej Równiak, Anna Robak, Stanisław Szteyn, Krystyna Bogus-Nowakowska, Barbara Wasilewska, Janusz Najdzion

*Department of Comparative Anatomy, University of Warmia and Mazury, Olsztyn, Poland*

[Received 30 June 2005; Accepted 22 July 2005]

*The characteristic features of guinea pig amygdala (CA), as shown by volumetric comparisons of the individual nuclei, are the poor development of the basolateral (BL) and lateral olfactory tract (NLOT) nuclei as well as the strong formation of the lateral (LA) and basomedial (BM) nuclei. The central (CE), cortical (CO) and medial (ME) nuclei also appear to be well represented in this species. All these features are even more pronounced when the total number of neurons in the nuclei referred to was taken into consideration. A comparison of the densities of neurons in the individual nuclei with the mean numerical density of cells in the guinea pig CA indicates that the densities of neurons in LA, BL, BM, CE and CO are significantly lower than the mean ( $p < 0.05$ ), whereas in the ME and NLOT these values are significantly higher than the mean ( $p < 0.05$ ). It is noteworthy, that the densities of the neurons in CE and CO do not differ statistically from each other ( $p > 0.05$ ) and are significantly higher than the respective values in LA, BL and BM ( $p < 0.05$ ). Furthermore, a similar division of the guinea pig CA may to some extent be made using the size parameters of the amygdaloid neurons as a marker. Interestingly, the large neurons populate organised CA areas like LA, BL and BM less densely, whereas the small cells create ME and NLOT, where the neurons are densely arranged. CE and CO occupy intermediate positions, with the neurons similar in size to the mean for the guinea pig CA.*

**Key words:** amygdala, guinea pig, morphometric analysis, 3-D reconstructions

## INTRODUCTION

There are 2 types of investigative process used by neuroscientists to examine the amygdala (CA) and other brain structures. The first of these is qualitative research, which employs symbols and words to indicate the presence or absence of features or to categorise them into different types. This approach has been adopted by the overwhelming majority of investigations devoted to CA during the last century and has indeed given deep insight into the structure

and functions of this brain centre [5, 14, 17–19, 21, 30, 32, 34, 35, 38, 39, 41, 42, 53]. However, this kind of scientific investigation also has its limitations and dangerously weak points. For example, since qualitative data are not numerical, there is no opportunity to evaluate objective differences and similarities in the organisation of the brain structures studied. Moreover, since the nature of such data may be subjective and their interpretation dependent on the individual researcher, attempts at comparison

can sometimes lead to different and inconsistent conclusions [50]. The second type of investigative process is quantitative research, which employs numerical indicators to ascertain the relative sizes, numbers and densities of the brain structures studied and their constituents. While qualitative methods can supply a greater depth of information about the nature of the brain structure studied, the quantitative methods can provide a high level of measurement precision and statistical power. Since the results reported from quantitative research are only in numerical form, direct comparisons can be made and the relationships between them statistically verified without difficulty. Moreover, since the results are statistically reliable, quantitative research can reliably determine the differences and similarities between the brain structures investigated. For this reason quantitative data can be used successfully in comparative research on the brain structures in different species [4, 20, 47, 50, 51].

In spite of all the advantages of the quantitative methods mentioned above, they have so far only occasionally been used in anatomical studies on CA. Hardly anything, for example, is known about the size of individual nuclei in CA of most of the species studied. The only detailed volumetric relationships between various amygdaloid regions were those reported by Maksymowicz [36] in the dog, by Śmiałowski [54] in the macaque and by Równiak et al. [46] in the common shrew. The size parameters of the basolateral amygdala were described by Breathnach and Goldby [4] in the porpoise and by Berdel et al. [1] in the developing brain of the rat. The comparative volumetric studies of Stephan et al. [50–52] in insectivora and primates are the most extensive to date, although they are restricted to the larger areas of CA and not to the single nuclei. Of the individual amygdaloid structures only NLOT and the large-celled portion of BL were taken into consideration. The quantitative aspects of the cellular populations in CA are even more obscure. For instance, detailed data concerning the density of neurons in individual amygdaloid nuclei have only been given for the common shrew [46] and they are, to the best of our knowledge, not available for other species. The total number of neurons in CA has been studied so far in the common shrew [46] and selected structures of the rat CA [48]. The only known detailed morphometric studies concerning the size of CA neurons have been those performed by Dziewiątkowski et al. [9] in the rabbit and, more recently, by Równiak et al. [46] in the common shrew.

The aim of our study, therefore, was to give the first detailed morphometric characteristics of CA in the guinea pig. These raw data on the morphometric measurements of the amygdaloid nuclei and their neurons enable comparisons to be made with similar data obtained in other laboratories from the same species. They can also be used in interspecific comparisons [4, 50–52].

## MATERIAL AND METHODS

A total of 6 brains were used to study the morphometric parameters of CA in the guinea pig. All efforts were made to minimise both animal suffering and the number of animals used. The brains were removed from the skulls, embedded in paraffin and sectioned on the Leica microtome at a thickness of 50  $\mu\text{m}$  in the coronal plane.

All sections were analysed cytoarchitectonically and morphometrically with a calibrated image analysis system consisting of a computer equipped with morphometric software (Multi-Scan 8.2, Computer Scanning Systems, Poland) and a light microscope coupled with a digital camera (CM40P, VideoTronic, Germany). The sequence of operations performed on a single animal is described in detail below.

### 3-D reconstruction of CA

The microscopic fields were viewed at low magnification through a 5-fold objective. The 512  $\times$  512 pixel microscopic images of a single section were digitally recorded by means of a camera coupled to a microscope and a computer. The scans were subsequently joined together to form larger areas comprising the whole CA and adjoining structures (so-called "digital slices"). Every second section in the series of microtome scraps available was taken into account.

The digital slices were registered by means of TPS (USA) and Morpheus (USA) morphometric software according to the Generalized Procrustes Analysis (GPA) that superimposes the landmark configurations using least squares estimates for the translation and rotation parameters [2, 11, 43, 44]. For more detailed information concerning the recording process used in the present study see our previous paper in this series [46].

All the registered digital slices of CA recorded from a single animal were incorporated into one multi-sliced 3-D image (a so-called "stack"). In this kind of 3-D data set the digital slices were the consecutive serial sections oriented perpendicular to the long axis of CA and covering the whole rostrocaudal extent of it. On each digital slice the boundaries of

the individual amygdaloid nuclei were outlined in different colours by a mouse-driven cursor. All the outlines were drawn under the control of the light microscope. The definite stack was then composed of the serially aligned raw images and the outlined structures of CA incorporated. With the help of IGL Trace software the 2-D outlines were transformed into 3-D slabs. The 3-D reconstruction of CA for a single animal was simply the sum of all the serially aligned slabs.

### Volumetric analysis

In order to evaluate the volume of the individual amygdaloid nuclei, the volumes of slabs traced with the same colour were totalled according to the formula proposed by Cavaliero [12, 26]. The total CA volume presented in this study was the sum of the volumes of the 7 amygdaloid nuclei studied, namely the lateral, basolateral, basomedial, central, cortical, medial and lateral olfactory tract nuclei.

### Numerical density counts

To evaluate the numerical density of cells in each of the amygdaloid nuclei, the optical dissector method was implemented using the guidelines described by West and Gundersen [56].

### Evaluation of the total number of neurons

The total number of neurons in each of the nuclei studied was calculated by multiplying the volume of the given nucleus by the numerical density of the cells in it [56].

### The morphometric parameters of the neurons

In each of the individuals studied a morphometric analysis of CA neurons was performed using Multi-Scan 8.2 morphometric software. Each neuron was characterised by a set of morphometric parameters: the length (the long axis of the soma), the width (the short axis of the soma), the size (the sum of both axes) and the shape factor (the ratio of both axes). The test frames were arranged so as to cover the total cross-sectional area of the nucleus studied. In the guinea pig 5 cross-sections per nucleus in the single animal were taken into account.

### Statistical analysis

The statistical analysis was performed using CSS: Statistica v.5.0 (Statsoft, USA). The analysis of variance (ANOVA) was performed followed by post hoc tests (Duncan's post hoc analysis) and planned comparison tests (Student's paired t-test) between the consecutive pairs of means. The level of statistical significance was set at  $p < 0.05$ . In order to evalu-

ate the precision of all measurements, the coefficient of error was calculated. Values below 0.1 were achieved for all the parameters examined.

## RESULTS

### The nuclear pattern of the guinea pig CA

The position of the various amygdaloid nuclei in the guinea pig CA and the pattern of their delimitation are shown in Figures 1 and 2 respectively.

As in other mammalian species, CA of the guinea pig is really 3 collections of nuclei. The largest and the best differentiated portion of CA is the basolateral nuclear group (BLC), consisting of the lateral (LA), basolateral (BL) and basomedial (BM) nuclei. The second is the central group (CC), composed of the anterior amygdaloid area (AAA) as well as the central (CE) and intercalated nuclei (I). The third portion of CA is the corticomедial group (CMC), formed by the cortical (CO) and medial nuclei (ME) as well as the nucleus of the olfactory tract (NLOT) and the amygdalohippocampal area (AHA).

The general morphology and cellular structure of these different amygdaloid regions in the guinea pig CA and their parcellation into the finer parts are very similar to those of the other rodents [21, 49]. Briefly, on the basis of more subtle differences in the density and cell size within LA, BL and BM, they can be further subdivided into the anterior (LAa, BLa and BMa) and posterior (LAp, BLp and Bmp) parts. Two subdivisions are also present within CE, although the boundaries between them are not as clear-cut as in the basolateral nuclei. The medial part (CEm) is located more rostrally and is composed of the larger, darker and more tightly-packed cells. The lateral part (CEl) contains the smaller, lighter and more loosely arranged neurons. In ME it is also possible to distinguish 2 regions, according to differences in the density and size of the cells. The anterior part (MEa) forms the rostral and main body of the nucleus, whereas the posterior part (MEp) constitutes the small thin caudal portion. Finally, CO consists of 3 distinct regions: the anterior cortical nucleus (COa), the periamygdaloid cortex (COc) and the posterior cortical nucleus (COp).

Although the borders of the various nuclei in the guinea pig CA were generally easy to recognise, not all these nuclear masses are equally separate and discrete. Some are poorly delineated in relation to the surrounding nuclei and so are not amenable to precise measurements. Owing to general delimitation problems, such structures as AAA, AHA and I were excluded from the volumetric investigation in

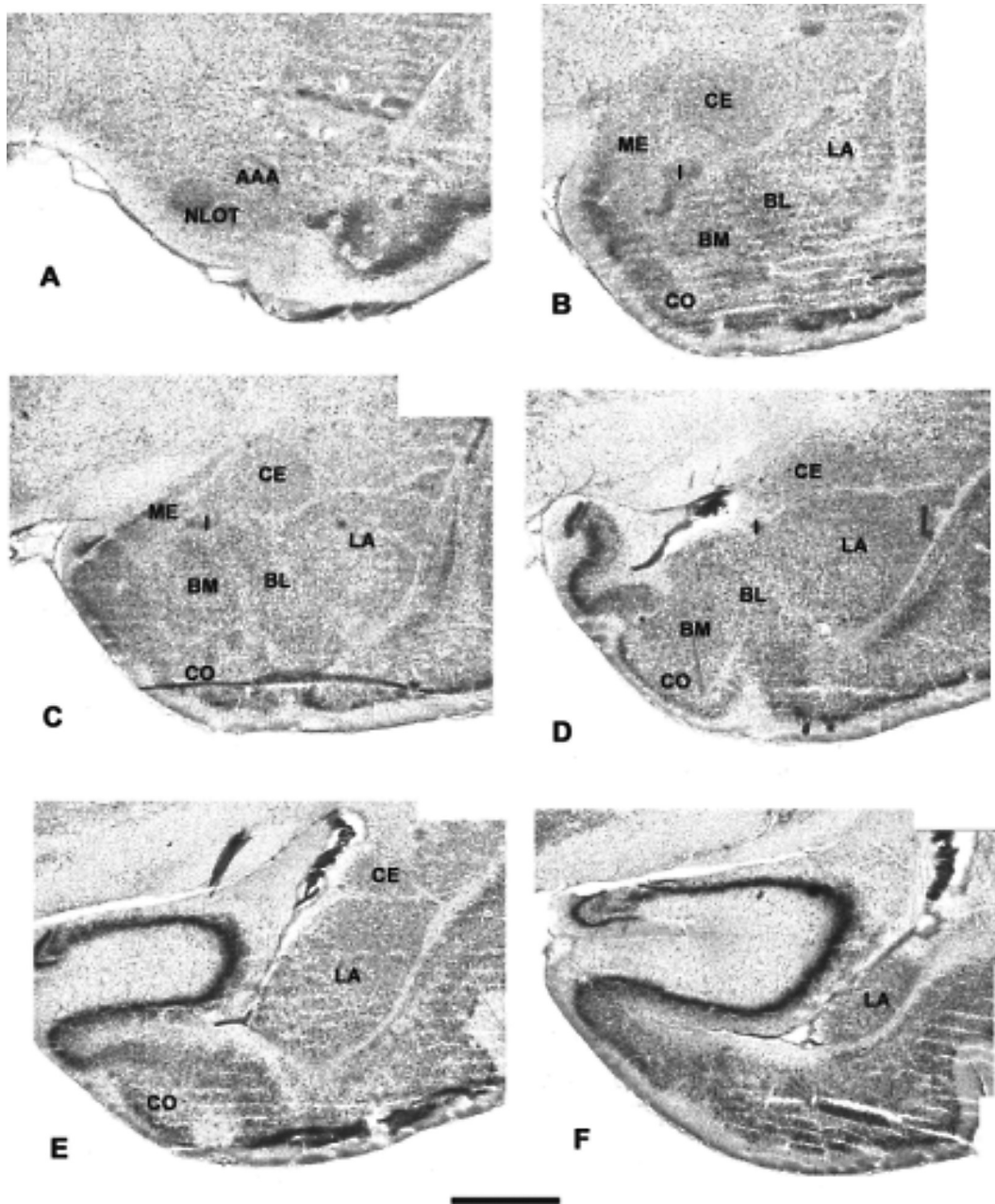


**Figure 1.** The position of the various amygdaloid nuclei in the guinea pig CA. A–F. The subsequent coronal sections through the guinea pig CA in the rostrocaudal direction. Scale bar: 1 mm.

the present study. The minor difficulties which were encountered in delineating the boundary between BM and CO, as well as the rostral borders of ME and CE, were overcome by taking into consideration the borders in the adjacent sections. Since all sections are serially aligned, the additional support in delineating the obscure portions in the guinea pig CA provided thick digital sections (200–300  $\mu\text{m}$ ) composed from single 50- $\mu\text{m}$  scraps.

#### The morphometric parameters of CA of the guinea pig

The morphometric data concerning individual CA nuclei are listed in the respective rows of Table 1. The values for CA as a whole are presented in the last row.

**Volume.** The characteristic features of the guinea pig CA are poor development of BL and NLOT, while LA and BM are, in contrast, strongly formed.

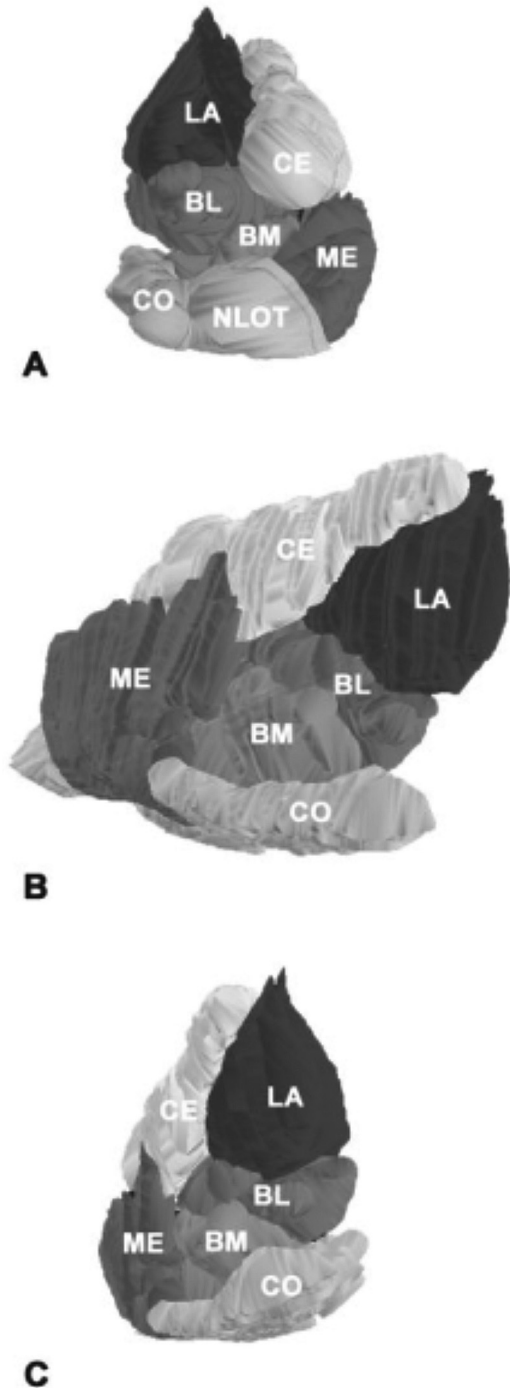


**Figure 2.** 3-D reconstruction of the guinea pig CA: **A–C.** Rostral, posteromedial and caudal views, respectively.

CE, CO and ME also appear well preserved in this species. The smallest average volume in the guinea pig's CA is that of NLOT, while the largest is that of LA. According to the raw volumetric measurements and percentages, almost all the nuclei studied are significantly different ( $p < 0.05$ ), although CE does not differ statistically from ME ( $p > 0.05$ ).

**Numerical density.** The density of neurons in the guinea pig CA is smallest in BL, while that in NLOT is the largest. Comparison of the densities of cells in the individual amygdaloid nuclei with the average for the total CA reveals that the densities of neurons in LA, BL, BM, CE and CO are significantly lower than the mean ( $p < 0.05$ ), whereas in ME and NLOT these values are significantly higher than the mean ( $p < 0.05$ ). It should be noted, however, that the density of neurons in CE does not differ significantly from that in CO ( $p > 0.05$ ). The density of cells in ME is also statistically similar to that in NLOT ( $p > 0.05$ ).

**The total number of neurons.** The smallest number of neurons in the guinea pig's CA is in NLOT, whereas the largest cellular population is in LA. According to the raw measurements and percentages, all the nuclei studied are indeed different ( $p < 0.05$ ).

**The morphometric parameters of neurons in the guinea pig CA**

The morphometric parameters of neurons in particular CA nuclei are listed in the respective rows of Table 2. The mean values for CA are presented in the last row.

**Neuron length.** The smallest average length of the soma in the guinea pig CA is displayed by the neurons located in the I, whilst the cells in BL are the longest. The average lengths of neurons in LA, BL, BM and CO are significantly higher than the length of the mean CA neuron ( $p < 0.05$ ). This value in CE does not differ statistically from the mean ( $p > 0.21$ ). In the remaining nuclei the average lengths of neurons are significantly lower than the mean ( $p < 0.05$ ). According to this parameter, almost all the nuclei studied are significantly different ( $p < 0.05$ ), although CE does not differ statistically from CO ( $p > 0.05$ ).

**Neuron width.** The smallest average width of the soma in the guinea pig CA is displayed by the cells in the I, whereas the largest perikarya, according to this parameter, are present in BL. The average widths of neurons in LA, BL and BM are significantly higher than the width of the mean CA neuron ( $p < 0.05$ ). This value in CO does not differ statistically from the mean ( $p > 0.95$ ). In the remaining nuclei these values are significantly lower than the mean ( $p < 0.05$ ). According to this parameter almost all the nuclei studied are significantly different ( $p < 0.05$ ), although LA does not differ statistically from BM ( $p > 0.05$ ), nor ME from NLOT ( $p > 0.05$ ).

**The average size of neurons.** The size of a neuron in the guinea pig CA was expressed in the present

**Table 1.** The morphometric parameters of the individual amygdaloid nuclei of the guinea pig CA

Nucleus	Volume [mm <sup>3</sup> ]	Percentage of volume (%)	Numerical density [N/mm <sup>3</sup> ]	Total number of neurons [N]	Percentage of neurons (%)
LA	2.76 ± 0.33	27.9 ± 1.1	75081.79 ± 1937.53	207182.5 ± 21766.86	24.31 ± 1.2
BL	1.53 ± 0.19	15.48 ± 0.97	49678.22 ± 1281.97	76092.36 ± 9393.15	8.93 ± 0.76
BM	0.96 ± 0.1	9.68 ± 0.17	66600.23 ± 1718.65	63752.51 ± 6425.22	7.48 ± 0.23
CE	1.4 ± 0.11	14.13 ± 0.68	90428.49 ± 2333.56	127667.8 ± 9853.41	15.01 ± 0.84
CO	1.7 ± 0.16	17.2 ± 0.62	91527.05 ± 2074.29	154063.7 ± 18224.75	18.06 ± 0.87
ME	1.28 ± 0.08	13.04 ± 0.93	144431 ± 3727.12	185700.3 ± 16336.36	21.84 ± 1.48
NLOT	0.25 ± 0.02	2.57 ± 0.14	146480.5 ± 3999.94	37076.39 ± 1887.17	4.36 ± 0.17
CA	9.89 ± 0.88	100 ± 0	94889.62 ± 804.13	851535.6 ± 69593.96	100 ± 0

**Table 2.** Morphometric parameters of the neurons in the individual amygdaloid nuclei of the guinea pig CA

Nucleus	Neuron length [μm]	Neuron width [μm]	Neuron size [μm]	Neuron shape
LA	15.75 ± 0.34	11.25 ± 0.67	27 ± 0.99	1.4 ± 0.05
BL	17.41 ± 0.39	12.59 ± 0.48	30 ± 0.85	1.38 ± 0.02
BM	15.21 ± 0.21	11.13 ± 0.25	26.34 ± 0.46	1.37 ± 0.02
CE	14.44 ± 0.57	9.44 ± 0.16	23.87 ± 0.48	1.53 ± 0.09
CO	14.56 ± 0.25	9.79 ± 0.39	24.36 ± 0.62	1.49 ± 0.05
I	10.51 ± 0.18	7.37 ± 0.34	17.88 ± 0.44	1.43 ± 0.07
ME	12.4 ± 0.18	8.27 ± 0.71	20.67 ± 0.85	1.5 ± 0.11
NLOT	14.19 ± 0.85	8.44 ± 0.34	22.64 ± 1.17	1.68 ± 0.02
CA	14.31 ± 2.09	9.79 ± 1.77	24.10 ± 3.80	1.47 ± 0.10

study as the sum of the length and width of the soma. The smallest size values in the guinea pig CA are found in the cells in the I. The neurons in BL are the largest. The average sizes of neurons in LA, BL and BM are significantly higher than the size of the mean CA neuron ( $p < 0.05$ ). This value in CO does not differ statistically from the mean ( $p > 0.06$ ). In the remaining nuclei the average sizes of the neurons are significantly lower than that of the mean CA neuron ( $p < 0.05$ ). According to this parameter all the nuclei studied are significantly different ( $p < 0.05$ ).

**The shape of neurons.** The shape of a neuron in the guinea pig CA was expressed in the present study as the ratio of the length and width of its soma (the shape factor). The smallest average value of this coefficient was noted in BM, whereas the largest mean was observed in NLOT. The shape factor values in CE and NLOT are significantly higher than the mean value for the total guinea pig CA ( $p < 0.05$ ). In CO

( $p > 0.05$ ) and ME ( $p > 0.22$ ) these values do not differ statistically from the mean. In the remaining nuclei they are significantly lower than the mean ( $p < 0.05$ ). According to this parameter, almost all the nuclei studied show significant differences ( $p < 0.05$ ). However, LA does not differ statistically from the I ( $p > 0.05$ ), nor the BM from LA and BL ( $p > 0.05$ ) and ME from CE and CO.

To summarise the data presented in this study the nuclei series of the guinea pig CA have been presented according to the increasing values of the morphometric parameters (Table 3).

## DISCUSSION

This is the first investigation that provides a detailed morphometric analysis of the 8 nuclei in the guinea pig CA. To our knowledge, no morphometric data have been available to date concerning the volumes of the various amygdaloid regions and the

**Table 3.** The guinea pig CA nuclei series according to the increasing values of the morphometric parameters

Volume		NLOT	BM	ME	CE	BL	CO	LA
Numerical density of neurons		BL	BM	LA	CE	CO	ME	NLOT
Total number of neurons		NLOT	BM	BL	CE	CO	ME	LA
Neuron length	I	ME	NLOT	CE	CO	BM	LA	BL
Neuron width	I	ME	NLOT	CE	CO	BM	LA	BL
Neuron size	I	ME	NLOT	CE	CO	BM	LA	BL
Neuron shape	BM	BL	LA	I	CO	ME	CE	NLOT
	Min.	—————→						Max.

number, density and size of the neurons in the guinea pig CA.

**Volume.** All the nuclei observed in the guinea pig CA in the present study have also been described in the common shrew [46], mole [16], rat [21, 42], gerbil [49], guinea pig [15] rabbit [9, 14, 57], cat [17, 21, 40], dog [36], porpoise [4], bat [13], tree shrew [10], monkey [41, 50, 52, 54] and in humans [3, 7]. Moreover, the general morphology of these different amygdaloid regions in the guinea pig CA and their parcellation into finer parts are most similar to those found by Krettek and Price [21] in the rat. On the other hand, there are some peculiar features in the size and in the degree of differentiation of the different nuclei in the guinea pig CA when they are compared to their counterparts in the other species. Attention is drawn to some of these peculiarities.

The volumetric comparisons of the 3 parts of the CA (basolateral, central and corticomедial) as they were defined in the common shrew [46] and guinea pig (present results) indicate the substantial progression of the basolateral region in the guinea pig's CA, whereas the central and corticomедial areas in this species have undergone a reduction, more or less marked. For example, the volume of the BLC increases from an average of 38.66% in the common shrew to 53.06% in the guinea pig, CC undergoes mild size regression from an average of 17.97% to 14.13%, while the volume of CMC is markedly reduced from 43.37% to 32.81%. The data for the common shrew are those previously reported by us [46]. It should be noted that the substantial enlargement of BLC in the guinea pig CA follows from LA and BM size progression, since BL is notably reduced in this species (compare the present results and 46). On the other hand, the decline of CMC area in the guinea pig CA is caused, first of all, by the strong regression of NLOT. In both species ME and CO demonstrate only mild reduction and seem to be fairly consistent in

their proportionate size (compare the present results and 46).

In the dog CA BLC is even larger than in the guinea pig CA, whereas CC and CMC demonstrate further marked reduction (compare the present results and 36). Moreover, LA occupies proportionately a much larger part of the dog CA in comparison with that of the guinea pig, whereas CE, ME and NLOT display further strong regression in this species. Since BL and BM were incorporated by Maksymowicz [36] into a single structure, there is no possibility of evaluating the differences in size between the species. Interestingly, CO in both these species seems to be fairly constant in its proportionate size.

When the CA of the guinea pig is compared with that of the macaque [54], the size progression of BLC in the latter is obvious, whereas CC and CMC are even smaller than in the dog (compare 36 and 54). BLC size progression, noted in the macaque, is especially due to huge LA enlargement, although BL and BM also seem to be well developed in CA of this species [54]. On the other hand, CE as well as CO, ME and NLOT are considerably smaller than in the guinea pig CA, causing CC and CMC size regression (compare the present results and 54). It should be noted that CE, CO and NLOT are even smaller than in the dog (for comparisons see 36 and 54).

According to Stephan et al. [52] the size progression of the basolateral region of CA seems to reach its peak in humans, which corresponds well with the scheme of CA evolution presented above. However, direct comparisons between guinea pigs and humans are difficult to perform because there are no volumetric data concerning individual CA nuclei in the latter [52]. Moreover, the basolateral region in the work of Stephan et al. [52] was incorporated into CO.

To summarise, all these data when taken together, support the general impression reported by Crosby and Humphrey [8] that "the lateral, basal and

accessory basal nuclei occupy proportionately a much larger part of the human amygdaloid area. On the contrary the medial nucleus and nucleus of the lateral olfactory tract are relatively considerably reduced in man". CE and CO are fairly constant in their proportionate size in the shrew and in humans according to these authors [8].

**Numerical density.** Comparison of the density of neurons in the guinea pig CA with that in the common shrew [46] revealed a substantial decrease in cellular density in the former. The average density of neurons in the guinea pig CA is approximately only 2/5 that of the common shrew. The density decrease is greater in the basolateral nuclei than in the corticomедial amygdaloid regions. The phenomenon of the negative correlation between the size of the brain structure and the density of cells in it has previously been described by Morgane et al. [37] in the limbic cortex of several Cetacean species and by Kowiańska [20] in the claustra of various mammals. Interestingly, the pattern of density value distribution in the guinea pig CA seems to be very conservative, since it is almost identical with that found in the common shrew [46]. In the guinea pig CA, for example, the nuclei seriate, according to the increasing values of cell density, displays the following arrangement: BL, BM, LA, CE, CO, ME, NLOT. In the common shrew this arrangement is as follows: BL, BM, LA, CE, CO, NLOT, ME [46]. Moreover, in both these species LA, BL and BM form cellular regions in the CA characterised by density values significantly lower than the mean density of cells in CA. The ME and NLOT, in contrast, represent densely organised amygdaloid areas where the densities of the neurons are significantly higher than the mean. The densities of cells in CE and CO in CA of the guinea pig and common shrew lie between those of the two previously mentioned regions.

**The total number of neurons.** In spite of the substantial decrease in the density of neurons in the nuclei of the guinea pig CA, the total number of cells in each is greater and significantly higher than in their counterparts in the common shrew [46]. The average size of the cellular population in the guinea pig CA is about 5.3 times larger than that in CA of the common shrew [46]. It should be noted that the neuronal population size increases in the individual CA nuclei differ significantly, as shown by the percentages of cells in each in relation to the total CA. Since the numbers of neurons in the individual CA nuclei are the products of two simultaneously occurring processes (the volume increase of the nucle-

us and the reduction in the density of cells in it), we regard these percentages as displaying genuine changes that have taken place in CA of the guinea pig in comparison with that of the common shrew. For example, when the percentages of neurons in LA and BM of the guinea pig CA are directly compared with the respective values in the common shrew, a similar development is noted as in the volumetric comparisons. The alterations in population size in NLOT seem, however, to be less marked than the volumetric changes. On the other hand, regression of the population size in BL is much greater than its volume reduction. Moreover, the reduction in ME volume noted in the present study is not followed by reduction in its population size. The percentage of ME neurons in the guinea pig CA is even larger than in the common shrew. The relationships between the neuronal population sizes in CA of various mammalian species have not yet been described.

**The neuronal structure.** In all nuclei of the guinea pig CA the average neuron sizes are significantly higher than in the homologous regions of CA of the common shrew ( $p < 0.05$ ). The size of the average neuron in the guinea pig CA is 1.3 times larger than in the common shrew and this difference is statistically significant ( $p < 0.05$ ). The positive correlation between the size of the given brain structure and the size of the neurons in it was mentioned by Morgane et al. [37] in a comparative report concerning the limbic cortices of several Cetacean species but has never been verified statistically. Additional support for this thesis can be provided by the recent studies of Dziewiatkowski et al. [9] in the rabbit, since the neurons in this species are considerably larger than those in the guinea pig (present results) and common shrew [46]. On the other hand Kowiańska [20] was unable to find a similar correlation in comparative studies of the neuronal structure in the claustra of mammals. In spite of the size progression, the distribution of neurons according to size in the guinea pig CA is very similar to those described in the common shrew [46] and rabbit [9]. In all 3 species the large neurons occupy less densely populated nuclei in CA such as LA, BL and BM, whereas the smallest cells create ME and NLOT, where the neurons are densely arranged. CE and CO are populated by middle-sized cells and their packing densities in both these structures are between those of the previously mentioned regions. It should be noted that the negative correlation between the size of the neurons in the amygdaloid nuclei studied and their packing densities in these regions was described previously in the common shrew [46]



and this phenomenon also seems to be present in the guinea pig CA.

**Functional remarks.** Since according to Stephan et al. [51] “the comparative neuroanatomical investigations have demonstrated that the size of given brain structure is highly interrelated with the functional requirements of its habits” the question arises as to what the functional consequences are of the way in which CA is organised in the guinea pig?

LA is the major input region for the sensory related thalamic and cortical inputs directed to CA and projects back to these areas as well [21, 33, 42, 53]. It appears to be the major site of convergence of all non-olfactory sensory modalities, the visual [25, 31], auditory [22, 24, 25, 29, 45] and somatosensory [23, 25, 55]. The BM, which also has strong interrelationships with the sensory related thalamic and cortical areas [6, 23, 42], seems to be more related to the contextual information [25, 27, 28]. Since both these nuclei are much better developed in the guinea pig CA in comparison with that of the common shrew [46], it is reasonable to state that non-olfactory information processed by the cortex becomes more widely represented inside CA of this species. These circumstances may therefore suggest that CA of the guinea pig is probably less influenced by olfaction. That seems not to be the case. ME and CO, which include the secondary olfactory and vomeronasal areas [18, 19, 53], have in fact undergone only a slight reduction in size in the guinea pig CA in comparison with the common shrew, so that olfaction would still appear to be very important in CA of this species. On the other hand, the sharp reduction in NLOT indicates that some olfactory regions, at least, are less important in the guinea pig CA.

## REFERENCES

- Berdel B, Moryś J, Maciejewska B, Dziewiątkowski J (1997) Volume and topographical changes of the basolateral complex during the development of the rat's amygdaloid body. *Folia Morphol*, 56: 1–11.
- Bookstein FL (1986) Size and shape spaces for landmark data in two dimensions. *Statistical Scie*, 1: 181–222.
- Braak H, Braak E (1983) Neuronal types in the basolateral amygdaloid nuclei of man. *Brain Res Bull*, 11: 349–365.
- Breathnach AS, Goldby F (1954) The amygdaloid nuclei, hippocampus and other parts of rhinencephalon in the porpoise (*Phocaena phocaena*). *J Anat*, 88: 267–291.
- Caffe AR, van Leeuwen FW, Luiten PG (1987) Vasopressin cells in the medial amygdala of the rat project to the lateral septum and ventral hippocampus. *J Comp Neurol*, 261: 237–252.
- Canteras NS, Swanson LW (1992) Projections of the ventral subiculum to the amygdala, septum and hypothalamus: A PHAL anterograde track-tracing study in the rat. *J Comp Neurol*, 324: 180–194.
- Crosby EC, Humphrey T (1941) Studies on the vertebrate telencephalon. II. The nuclear pattern of olfactory nucleus, tuberculum olfactorium and the amygdaloid complex in adult man. *J Comp Neurol*, 74: 309–352.
- Crosby EC, Humphrey T (1944) Studies on the vertebrate telencephalon. III. The amygdaloid complex in the shrew (*Blarina brevicauda*). *J Comp Neurol*, 81: 285–305.
- Dziewiątkowski J, Berdel B, Kowiański P, Kubasik-Juraniec J, Bobek-Bilewicz B, Moryś J (1998) The amygdaloid body of the rabbit — a morphometric study using image analyser. *Folia Morphol*, 57: 93–103.
- Flugge G, Ahrens O, Fuchs E (1994) Monoamine receptors in the amygdaloid complex of the tree shrew (*Tupaia belangeri*). *J Comp Neurol*, 343: 597–608.
- Gower JC (1975) Generalized Procrustes analysis. *Psychometrika*, 40: 33–51.
- Gundersen HJG, Jensen EB (1987) The efficiency of systematic sampling in stereology and its prediction. *J Microsc*, 147: 229–263.
- Humphrey T (1936) The telencephalon of the bat. I. The non-cortical nuclear masses and certain pertinent fiber connections. *J Comp Neurol*, 65: 603–711.
- Jagalska-Majewska H, Dziewiątkowski J, Wójcik S, Luczyńska A, Kurlapska R, Moryś J (2001) The amygdaloid complex of the rabbit — a morphological and histochemical study. *Folia Morphol*, 60: 259–280.
- Johnson TN (1957a) Studies on the brain of a guinea pig. I. The nuclear pattern of certain basal telencephalic centers. *J Comp Neurol*, 107: 353–477.
- Johnson TN (1957b) The olfactory centers and connections in the cerebral hemisphere of the mole (*Scalonus aquaticus machrinus*). *J Comp Neurol*, 107: 379–425.
- Kamal AM, Tombol T (1975) Golgi studies on the amygdaloid nuclei of the cat. *J Hirnforsch*, 16: 175–201.
- Kevetter GA, Winans SS (1981) Connections of the Corticomedial Amygdala in the Golden Hamster. I. Efferents of the “Vomeronasal Amygdala”. *J Comp Neurol*, 197: 81–98.
- Kevetter GA, Winans SS (1981) Connections of the Corticomedial Amygdala in the Golden Hamster. II. Efferents of the “Olfactory Amygdala”. *J Comp Neurol*, 197: 99–111.
- Kowiańska J (1997) Anatomia porównawcza przedmurza wybranych gatunków ssaków. PhD Thesis, Medical University, Gdańsk, pp. 1–107.
- Krettek JE, Price JL (1978b) A description of the amygdaloid complex in the rat and cat with observations on intra-amygdaloid axonal connections. *J Comp Neurol*, 178: 255–280.
- LeDoux JE, Farb C, Ruggiero DA (1990b) Topographic organization of neurons in the acoustic thalamus that project to the amygdala. *J Neurosci*, 10: 1043–1054.
- LeDoux JE, Cicchetti P, Xagoranis A, Romanski LM (1990a) The lateral amygdaloid nucleus: sensory interface of the amygdala in fear conditioning. *J Neurosci*, 10: 1062–1069.
- LeDoux JE, Farb C, Ruggiero DA (1991) Overlapping projections to the amygdala and striatum from audi-

- tory processing areas of the thalamus and cortex. *Neurosci Lett*, 134: 139–144.
25. LeDoux JE (2000) Emotion circuits in the brain. *Annu Rev Neurosci*, 23: 155–184.
  26. Mayhew TM (1992) A review of recent advances in stereology for quantifying neural structures. *J Neurocytol*, 21: 313–328.
  27. Majidishad P, Pelli DG, LeDoux JE (1996) Disruption of fear conditioning to contextual stimuli but not to a tone by lesions of the accessory basal nucleus of the amygdala. *Soc. Neurosci. Abstr.* 22: 1116.
  28. Maren S, Fanselow MS (1995) Synaptic plasticity in the basolateral amygdala induced by hippocampal formation stimulation in vivo. *J Neurosci*, 15: 7548–7564.
  29. Mascagni F, McDonald AJ, Coleman JR (1993) Corticoamygdaloid and corticocortical projections of the rat temporal cortex: a Phaseolus vulgaris leucoagglutinin study. *Neuroscience*, 57: 697–715.
  30. McDonald AJ (1985) Morphology of peptide-containing neurons in the rat basolateral amygdaloid nucleus. *Brain Res*, 338: 186–191.
  31. McDonald AJ, Jackson TR (1987) Amygdaloid connections with posterior insular and temporal cortical areas in the rat. *J Comp Neurol*, 262: 59–77.
  32. McDonald AJ, Pearson JC (1989) Coexistence of GABA and peptide immunoreactivity in non-pyramidal neurons of the basolateral amygdala. *Neurosci. Lett*, 100: 53–58.
  33. McDonald AJ, Mascagni F, Guo L (1996) Projections of the medial and lateral prefrontal cortices to the amygdala: A Phaseolus vulgaris leucoagglutinin study in the rat. *Neuroscience*, 71: 55–75.
  34. McDonald AJ (1996) Glutamate and aspartate immunoreactive neurons of the rat basolateral amygdala: colocalization of excitatory amino acids and projections to the limbic circuit. *J Comp Neurol*, 365: 367–379.
  35. McDonald AJ, Mascagni F (2001) Colocalization of calcium-binding proteins and GABA in neurons of the rat basolateral amygdala. *Neuroscience*, 105: 681–693.
  36. Maksymowicz K (1963) Amygdaloid complex of the dog. *Acta Biol. exp. Vars*, 23: 63–73.
  37. Morgane PJ, McFarland WL, Jacobs MS (1982) The limbic lobe of the Dolphin brain: A quantitative cytoarchitectonic study. *J. Hirnforsch*, 23: 465–552.
  38. Moga MM, Gray TS (1985) Peptidergic efferents from the intercalated nuclei of the amygdala to the parabrachial nucleus in the rat. *Neurosci Lett*, 61: 13–18.
  39. Moryś J, Berdel B, Jagalska-Majewska H, Luczynska A (1999) The basolateral amygdaloid complex — its development, morphology and functions. *Folia Morphol*, 58: 29–46.
  40. Pare D, Smith Y (1993) Distribution of GABA immunoreactivity in the amygdaloid complex of the cat. *Neuroscience*, 57: 1061–1076.
  41. Pitkänen A, Amaral DG (1994) The distribution of GABA-ergic cells, fibers, and terminals in the monkey amygdaloid complex: An immunohistochemical and in situ hybridization study. *J Neurosci*, 14: 2200–2224.
  42. Pitkänen A, Jolkkonen E, Kempainen S (2000) Anatomical heterogeneity of the rat amygdaloid complex. *Folia Morphol*, 59: 1–23.
  43. Rohlf FJ, Slice DE (1990) Extensions of the Procrustes method for the optimal superimposition of landmarks. *Systematic Zool*, 39: 40–59.
  44. Rohlf FJ (1999) Shape statistics: Procrustes superimpositions and tangent spaces. *J Classification*, 16: 197–223.
  45. Romanski LM, LeDoux JE (1993) Information cascade from primary auditory cortex to the amygdala: Corticocortical and corticoamygdaloid projections of temporal cortex in the rat. *Cereb Cortex*, 3: 515–532.
  46. Równiak M, Sztejn S, Robak A (2004) The morphometric study of the amygdala in the common shrew. *Folia Morphol*, 63: 165–176.
  47. Równiak M (2002) Cytoarchitektonika i analiza jąder ciała migdałowatego u wybranych gatunków ssaków łozyskowych. PhD Thesis, Medical University of Gdańsk, pp. 1–95.
  48. Salmenperä T, Kälviäinen R, Partanen K (2000) MRI volumetry of the hippocampus, amygdala, entorhinal cortex, and perirhinal cortex after status epilepticus. *Epilepsy Res*, 40: 155–170.
  49. Salter CF (1975) A morphological study of the lateral olfactory areas of the telencephalon in the Mongolian Gerbil, *Meriones unguiculatus*. *J Hirnforsch*, 16: 223–244.
  50. Stephan H, Andy OJ (1977) Quantitative comparisons of the amygdala in insectivores and primates *Acta Anat*, 98: 130–153
  51. Stephan H, Frahm H, Baron G (1981a) New and revised data on volumes of brain structures in insectivores and primates *Folia Primatol*, 35: 1–29
  52. Stephan H, Frahm H, Baron G (1987) Comparisons of brain structure volumes in insectivora and primates. VII Amygdaloid body *J Hirnforsch*, 28: 571–584
  53. Swanson LW, Petrovich GD (1998) What is the amygdala? *Trends Neurosci*, 21: 323–31.
  54. Śmiałowski A (1965) Amygdaloid complex of the macaque. *Acta Biol. Exp Vars*, 25: 77–89.
  55. Turner BH, Zimmer J (1984) The architecture and some of the interconnections of the rat's amygdala and lateral periallocortex. *J Comp Neurol*, 227: 540–557.
  56. West MJ, Gundersen HJG (1990) Unbiased stereological estimation of the number of neurons in the human hippocampus. *J Comp Neurol*, 296: 1–22.
  57. Young MW (1936) The nuclear pattern and fiber connections of the non-cortical centers of the telencephalon of the rabbit (*Lepus cuniculus*). *J Comp Neurol*, 65: 295–401.